Applied Physics B (2019) 125:30
https://doi.org/10.1007/s00340-019-7136-9

Applied Physics B
Lasers and Optics

16-Port tunable fiber laser based on a digital micromirror device in C-band

Jinliang Li[1] · Xiao Chen[1] · Min Lv[1] · Yunshu Gao[1] · Genxiang Chen[1]

Received: 23 October 2018 / Accepted: 9 January 2019 / Published online: 29 January 2019

Abstract
A 16-port tunable fiber laser is experimentally demonstrated based on a digital micromirror device (DMD). This laser has the capacity of tuning wavelength from 16 ports flexibly and independently in the whole C-band by only one 0.55-in. DMD chip, a blazed grating for waveband de-multiplexing and a zoom optics system for beam mapping. The results show the outputs from all fiber rings exhibit high uniformity, stability and reliability. The 3-dB linewidth of laser output is less than 0.02 nm, the SMSR exceeds 50 dB and the crosstalk between wavelength channels from adjacent ports is up to 45 dB. The wavelength shift is below 0.02 nm and the output power fluctuation is better than 0.13 dB within 1 h. This multi-port tunable fiber laser is expected to play the role of 16 or even more independent tunable lasers in network application.

1 Introduction

With the development of laser technology in the fields of communications, sensing, biomedicine, instrument testing and automation, the demands for tunable fiber lasers have grown rapidly in recent years due to the advantages including narrow linewidth, low-intensity noise, and compatibility with fiber optics. Tunable fiber lasers can not only replace multiple fixed-wavelength lasers, but also play dominant roles in many new laser systems. For example, in dense wavelength division multiplexing (DWDM) systems, multi-wavelength-tunable lasers not only greatly reduce the cost of system operation, maintenance and backup, but also realize the remote dynamic allocation of network resources. Additionally, tunable lasers have significant potential applications in other domains, such as optical RF transmission systems, all-optical wavelength conversion, wavelength routing, optical packet data exchange, and wavelength-based personal virtual networks. Therefore, multi-wavelength-tunable fiber lasers have attracted considerable interest from researchers and network service vendors.

Up to now, the corresponding research has focused on how to achieve enough tunable wavelength channels and equalize power outputs from fiber lasers. Multi-wavelength filters are the key components in waveband selection. Several reported approaches to realize wavelength filters have been proposed, including optical fiber subrings and Sagnac rings [1–3], fiber Bragg gratings (FBGs) (Bragg gratings written on high-birefringence fibers, sampled Bragg gratings, few-mode fiber gratings) [4], Fabry–Perot or etalon filters [5–7], acousto-optic tunable filters [8], Mach–Zehnder interferometers based on optical waveguides [9] and LCoS-SLM [10–12]. For example, Chien adopted a fiber optic reflector and tunable band-pass filter to establish tunable F–P cavity fiber lasers. The tuning range was 1533.75–1560.95 nm and the side-mode suppression ratio (SMSR) was greater than 40dB [7]. Alameh et al. proposed a single-unit C-band tunable laser based on an LCoS-SLM. A single-longitudinal mode tunable fiber laser was demonstrated with the SMSR greater than 35 dB and laser linewidth of 0.05 nm. The power uniformity was better than 0.25 dB [13].

Based on the previous research [14, 15], we propose and demonstrate a 16-port wavelength-tunable fiber laser based on a 0.55-in. DMD chip in this paper. A digital micromirror device (DMD) is used as a programmable filter and an erbium-doped fiber amplifier (EDFA) acting as the gain medium. By compact zoom optical system, a DMD chip is effectively utilized and flexibly tunes multi-wavelengths in the whole C-band from 16 fiber rings independently. Compared with the previous work, the system increases the number of ports for laser output and the utilization of the DMD working area. Experimental results show that the outputs from all units demonstrate high uniformity and stability. The

✉ Xiao Chen
xchen4399@126.com

[1] College of Science, MINZU University of China, Beijing 100081, People's Republic of China

3-dB linewidth is less than 0.02 nm and the tuning precision is 0.08 nm. The SMSR is up to 50 dB and the crosstalk between adjacent ports is better than 45 dB. Besides, the shift of the center wavelength is below 0.02 nm and the laser output power uniformity is around 0.13 dB within 1 h at room temperature.

2 Operation principle and system design

2.1 Principle of laser operation

Figure 1 shows the experimental setup of a 16-port tunable fiber laser. All 16 optical fiber-ring resonators share a unit of bulk optics. Each fiber loop includes an EDFA, a fiber coupler, a polarization controller (PC) and a circulator. The EDFA emits the C-band amplified spontaneous emission spectrum (ASE) signals. After a 90/10 fiber coupler, 90% ASE light energy returns into a ring and then continues to be coupled to bulk optics via a circulator and a fiber collimator array. The bulk optics consists of two lenses, a diffraction grating and a DMD chip. The fiber collimator array has 16 ports with the spacing of 1.2 mm, as shown in Fig. 2b. The fiber collimator array and the diffraction grating are located at the front and rear focal planes of lens 1 (focal length $f_1 = 300$ mm), respectively. In addition, the diffraction grating and the DMD are placed on the front and rear focal planes of the collimating lens 2 (focal length $f_2 = 100$ mm), respectively. The entire bulk optical system is a typical 4-f system.

The broadband ASE of 1530–1560 nm is de-multiplexed by the grating along different directions and aligned to map on the active window of the DMD as illustrated in Fig. 2a. By uploading steering holograms onto the DMD controlled by remote software, any waveband of ASE spectra can be routed and coupled to the optical system along the original

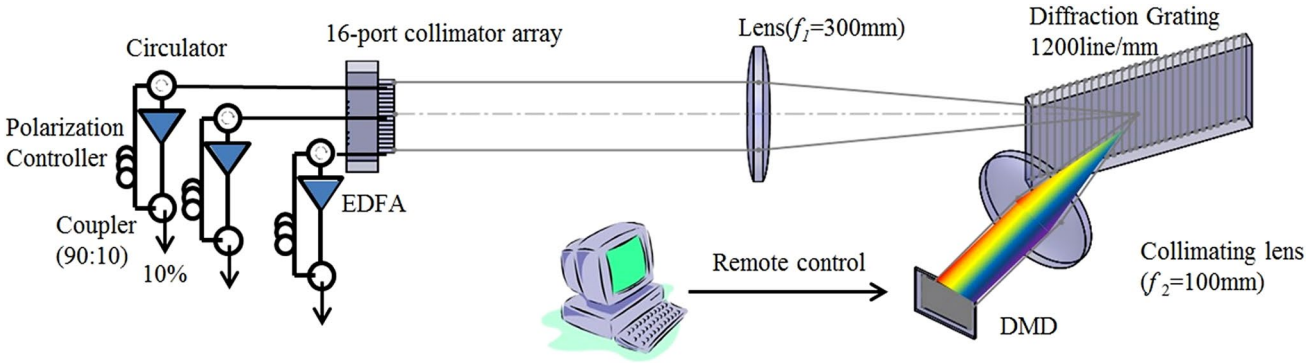

Fig. 1 Schematic diagram of the experimental setup

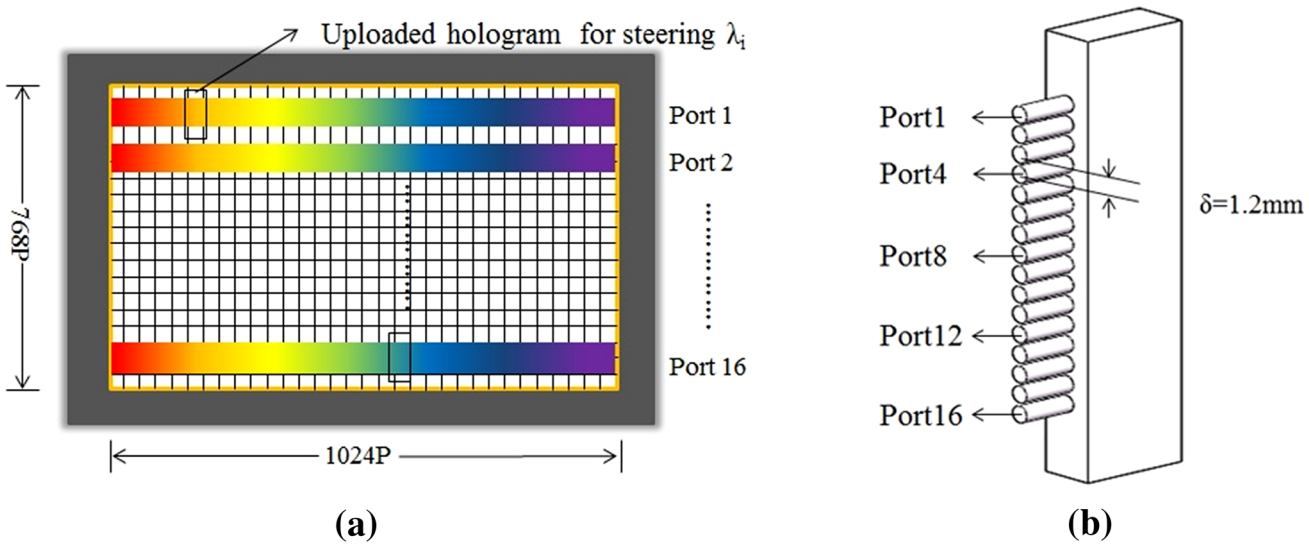

Fig. 2 Distribution of multiple ASE dispersion holograms on DMD (**a**) and the collimator array (**b**)

path, and the others are dropped out with dramatic attenuation, thereby realizing the laser longitudinal mode selection and wavelength tuning. The selected waveband through the collimator and circulator that returns to the ring cavity is amplified by the EDFA, leading, after several re-circulations, to high-quality lasing generation.

2.2 DMD diffraction

A DMD is an array of thousands of individually addressable and tiltable mirror pixels, manufactured by very large scale integration (VLSI) technology. These micromirrors driven by voltage can be independently tilted $\pm 12°$ along the diagonal, corresponding to an "on" or "off" state as shown in Fig. 3a. The diffraction performance of tilting micromirror array is the same with that of a 2D blazed grating.

In the tunable fiber laser, the configuration of a DMD must satisfy two basic conditions: (1) the light diffracted by a DMD should meet the near-blazed condition to reduce the insertion loss; (2) the wavelength channels selected by the DMD must route back into the system to build a closed loop. Therefore, based on the 2D grating model of a DMD (the detailed physical model refers to the reference [16]), we analyze the DMD diffraction characteristics in theory and further simulate it using VirtualLab Fusion software as well.

A 0.55-in. 1024×768-pixel DMD with the pitch of 10.8 μm is applied as a programmable filter in the laser system. Figure 3b1–d1 represents the diffraction distribution at the bisecting plane of the DMD when the light with a 1550-nm wavelength is incident at different angles. According to the grating theory, the principal maxima of multiple-pixel interference (blue peaks in Fig. 3) are modulated by the single-pixel diffraction envelope (red dash curves). Figure 3b2–d2 shows the corresponding diffraction patterns. The results show when the 1550-nm light is incident at an arbitrary angle, like $\alpha = 52°$, four distinct diffraction orders occur in space. Thus, the energy is not concentrated and the diffraction efficiency is lower than 11.4% on average, called off-blazed (http://www.ti.com/lit/wp/dlpa037/dlpa037.pdf). In Fig. 3c, when $\alpha = 24°$, the diffraction energy is mainly focused on the first order, and the diffraction efficiency is up to 65.9%, thus satisfying the ideal blazed condition. However, the diffracted beam cannot backtrack because the corresponding diffraction angle $\beta = 0°$ is away from the original path. Furthermore, when $\alpha = 12°$, Fig. 3d demonstrates that the diffraction energy is also concentrated and the efficiency is 65.4%. Besides, the diffraction order returns at $\beta = 12°$, exactly along the original path into the fiber ring. So $\alpha = 12°$ is an appropriate angle for the closed-loop tunable laser.

2.3 Optical system optimization

To maximum utilize the working area of the DMD to improve the diffraction efficiency, tuning accuracy and port counts, we calculate the ASE dispersion length covering the DMD, and further balance the width of 16 beams mapping on the DMD surface and the guard interval between adjacent ports to suppress the channel crosstalk. The dispersion length is determined by the grating and the collimator lens. We assume that the incident angles of beams from 16 ports

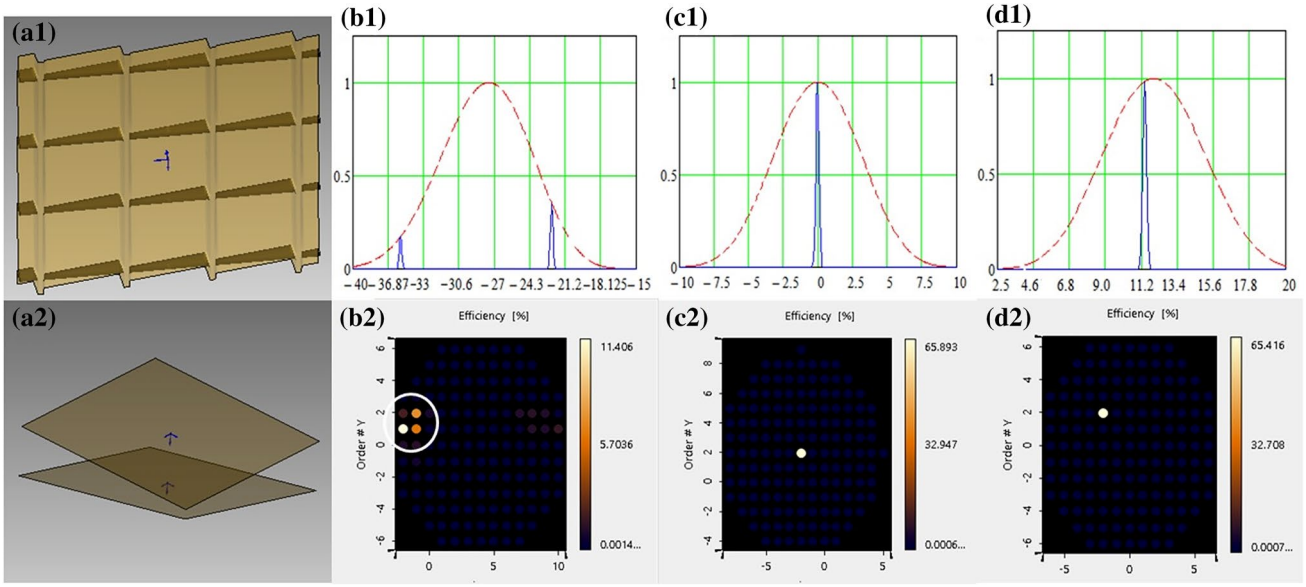

Fig. 3 **a** Schematic of the 12°-mirror-tilting DMD and the diffraction distribution of 1550-nm wavelength light radiating on a 0.55″ DMD at the bisecting plane with the incident angles 52° (**b1**), 24° (**c1**) and 12° (**d1**), respectively. (Red curves represent the single-pixel diffraction envelop and the blue curves are multi-pixel interference.) The corresponding diffraction patterns in space are shown in **b2–d2**

are all in the diffraction plane, so according to the grating equation:

$$d(\sin\alpha + \sin\beta) = k\lambda, \quad (1)$$

where k is the diffraction order (here only the first order is considered), d is a grating period of 1200 lines/mm, λ is the wavelength, and α and β are the incident angle and diffraction angle, respectively. The laser operates between 1530 nm and 1560 nm and $\alpha = 68°$ (the blazed angle of the grating), so that $\beta = 65.4°$@1530 nm and $\beta = 70.9°$@1560 nm. After the collimating lens ($f_2 = 100$ mm), the dispersion length aligned on the DMD is 9.9 mm. Figure 4 shows the dispersion spectrum on the DMD simulated by OpticStudio that the utilization ratio of the DMD in the horizontal axis is up to 90.2%.

The 16-port fiber collimator array in Fig. 2b is 19.2 mm in length with the spacing of 1.2 mm. The port arrangement is linearly mapped onto the DMD. Considering that the width of the DMD is 9.06 mm, the Gaussian spot diameter on the DMD is about 0.328 mm and enough guard intervals between adjacent ports, two lenses are adopted with the focal length of 300 mm and 100 mm to zoom the optical system. Thus, the 3:1 optical configuration ensures the utilization of the DMD active area in vertical axis to be 70.6%. In addition, we notice the wavelength positions from 16 ports on the DMD in Fig. 4 are slightly displaced, like crescent distribution. It is because the beams from 16 ports are all focused on the surface of a grating, so that the incident angle of 16 beams is slightly out of diffraction plane, leading to the dispersion displacement on the DMD.

It is important to note that this DMD-based optical architecture is capable to achieve 20-port lasers in maximum without the need for moving components or structures. That is to say, this 20-port tunable fiber laser plays the role of 20 independently tunable lasers, which makes it very attractive for commercialization. Furthermore, it is expected to support 32 ports or even more by increasing the port counts from the collimator array and the DMD size. Furthermore, the multi-port tunable laser system can also be extended to the 2-μm band, which has considerable potential applications in the biomedical domain [17, 18].

3 Experimental results and analysis

When the laser loop is open, the output is the signal of waveband selection from the DMD. The average insertion loss is measured to be around 12 dB by comparing the ASE noise from an EDFA and the signal of selected wavebands. The measured total loss in the laser system is mainly from (1) the polarization-dependent loss of the grating; (2) the diffraction losses from the DMD and grating; (3) the reflection loss of lenses; (4) the insertion loss of the circulator and collimator. In the open loop, the 3-dB linewidth of an output signal is around 0.40 nm by uploading an 8×32-pixel hologram to the DMD as shown in the inset of Fig. 5.

When the optical loop is closed, it is observed a typical lasing output in Fig. 5 after the pump power up to the threshold. The 3-dB linewidth of the lasing signal is less than 20 pm, which is limited by the resolution of the

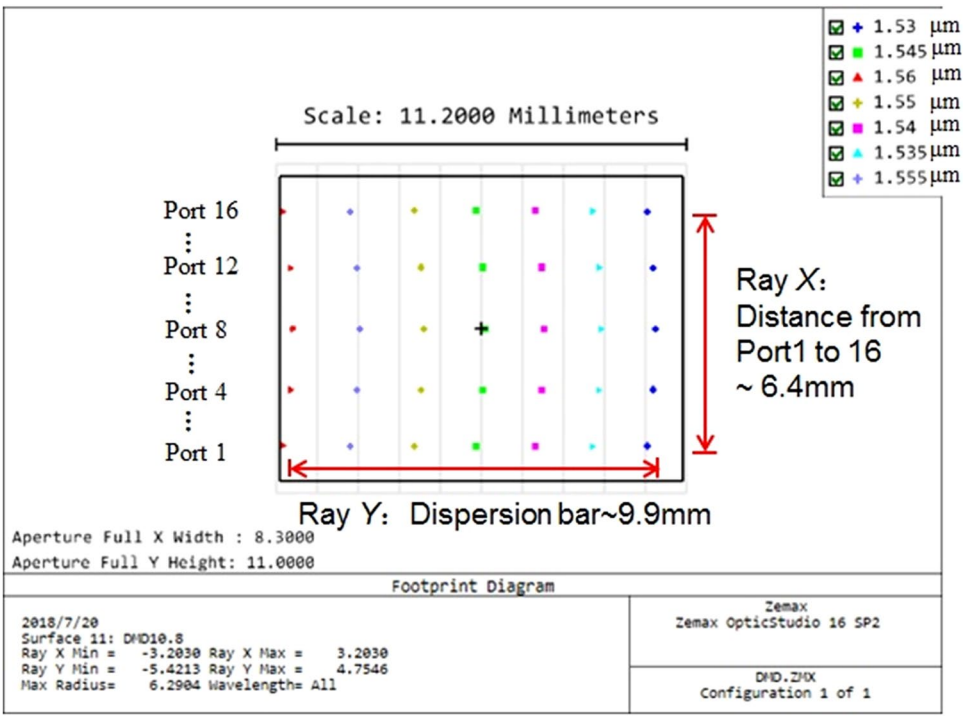

Fig. 4 Distribution of ASE dispersion spectrum from 16 ports mapped on a DMD

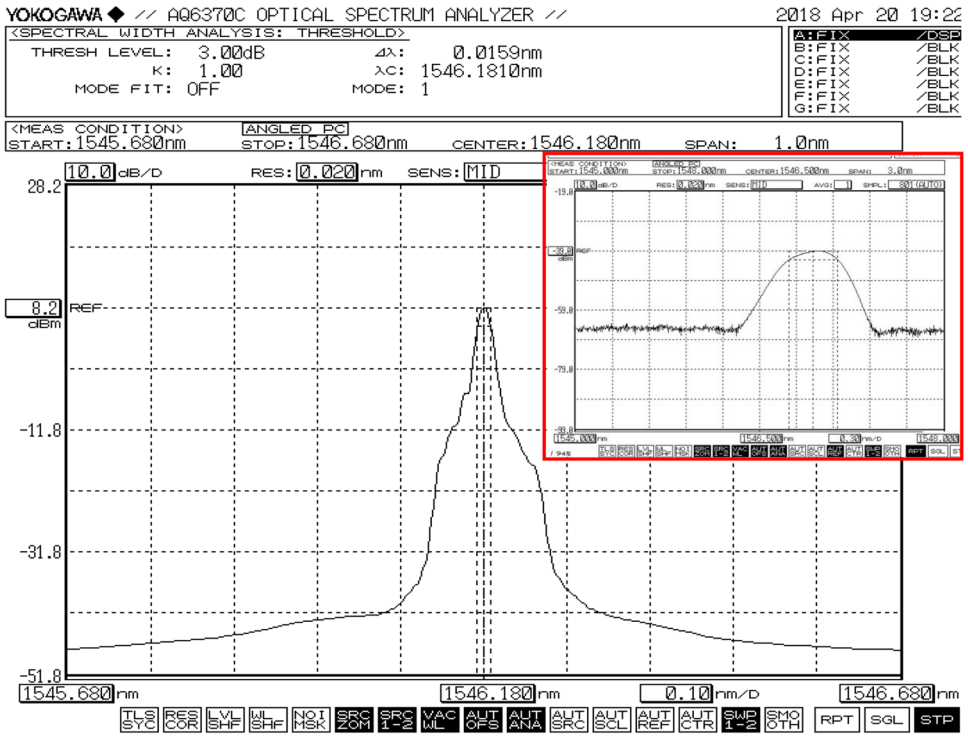

Fig. 5 Lasing output from the tunable fiber laser in the closed loop by uploading an 8×32-pixel hologram onto the DMD. The inset is the signal of waveband selection in the open loop

spectrum analyzer. The measured side-mode suppression ratio (SMSR) is greater than 50 dB and the laser output power is 8.2 dBm. Note that the lasing output in Fig. 5 is not a standard Lorentzian profile, but with shoulders on both sides of the spectrum. It is due to the multi-mode oscillation in the long cavity, so that the output signal shown in Fig. 5 is actually an envelope of the multi-mode superposition.

Figure 6a shows the dependence of measured signals from tunable fiber laser on the pump power from 1 to 4 mW. When the pump power is low, the emission spectrum is mainly characteristic of amplified spontaneous emission from an EDFA and waveband selection. At a kink at the threshold of 4 mW, the sharp peak occurs in spectrum and the linewidth becomes rapidly narrow. By further increasing the pump energy, this signal is dominated by the stimulated emission and the lasing is achieved as shown in Fig. 6b. So we know that the pump threshold power is about 4 mw, thus the laser slope efficiency is determined around 31%.

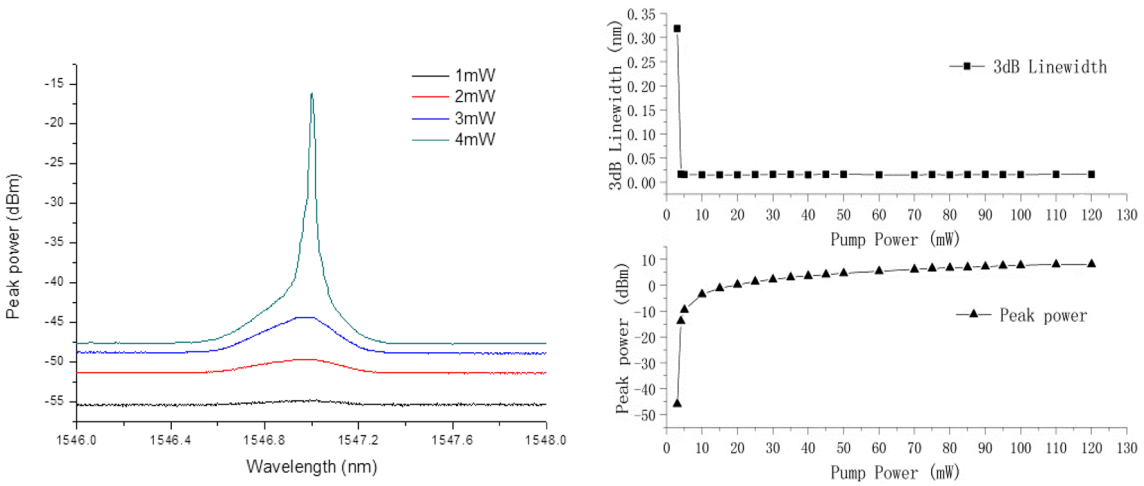

Fig. 6 **a** Measured signals of tunable fiber laser with the pump power from 1 to 4 mW. **b** Output power and 3-dB linewidth of signals as a function of the pump power in the closed loop

Figure 7 shows the lasing outputs at ports 1, 4, 8, 12, and 16, respectively. The measured outputs demonstrate the DMD-based fiber laser has an excellent tuning capability over the whole C-band through the generation of 8 × 32-pixel holograms at different positions along the DMD active window. It should be noted that the 16-laser beam alignments depend on the flatness of the ASE spectrum and the relative position of the DMD.

For the tuning accuracy, we define $R = p\,\Delta\lambda/L$, where $\Delta\lambda$ is 30 nm covering from 1530 to 1560 nm, L is the dispersion length 10.9 mm, and p is the single-pixel size, 10.8 μm. So the tuning accuracy R is calculated as 0.0297 nm/pixel. In the experiment, we move an 8 × 32-pixel hologram in a step of 3 pixels for fine-tuning. The tuning resolution is detected in an experiment around 0.08 nm displayed in Fig. 8f.

Figure 8 shows the drift of the wavelength (dotted line) and the fluctuation of peak power (solid line) at the pump power of 50 mW during 1-h observation at a center wavelength of 1545 nm. The maximum wavelength drift is less than 0.02 nm and the maximum fluctuation of peak power is 0.13 dB at the room temperature.

The crosstalk between the adjacent ports is an important specification of multi-port output laser. For the collimator port spacing is 1.2 mm and the zoom ratio of optical system is 3:1, the spectra spacing on the DMD is 0.4 mm. Figure 9 shows the crosstalk of the wavelength channels between adjacent ports in the tunable laser. When the pump power is 50 mW, the crosstalk of port 7 and port 9 is measured when port 8 output is defined as the lasing signal. The crosstalk between all laser ports is measured to be better than 45 dB.

4 Conclusions

A 16-port tunable fiber laser is proposed and experimentally demonstrated based on a DMD chip. The laser has the ability to independently, flexibly, and stably tune wavelengths in the whole C-band using only a single 0.55-inch DMD for multi-wavelength selection, a blazed grating for band de-multiplexing and zoom optics system for beam mapping. Based on the two-dimensional grating diffraction theory, the requirements for near-blazed condition of the DMD and the closed loop of the laser system are analyzed in detail. Experimental results show that the outputs from all fiber rings exhibit high uniformity and stability. For each port, the 3-dB linewidth of the laser output is less than 0.02 nm, the maximum output power is about 8.2 dBm, the SMSR exceeds 50 dB and the crosstalk between wavelength channels of adjacent ports is more than 45 dB. The fluctuation of the center wavelength is below 0.02 nm and the laser output power uniformity is better than 0.13 dB within 1 h at room temperature. This multi-port tunable fiber laser can replace a 16 or even more independent tunable lasers in optical

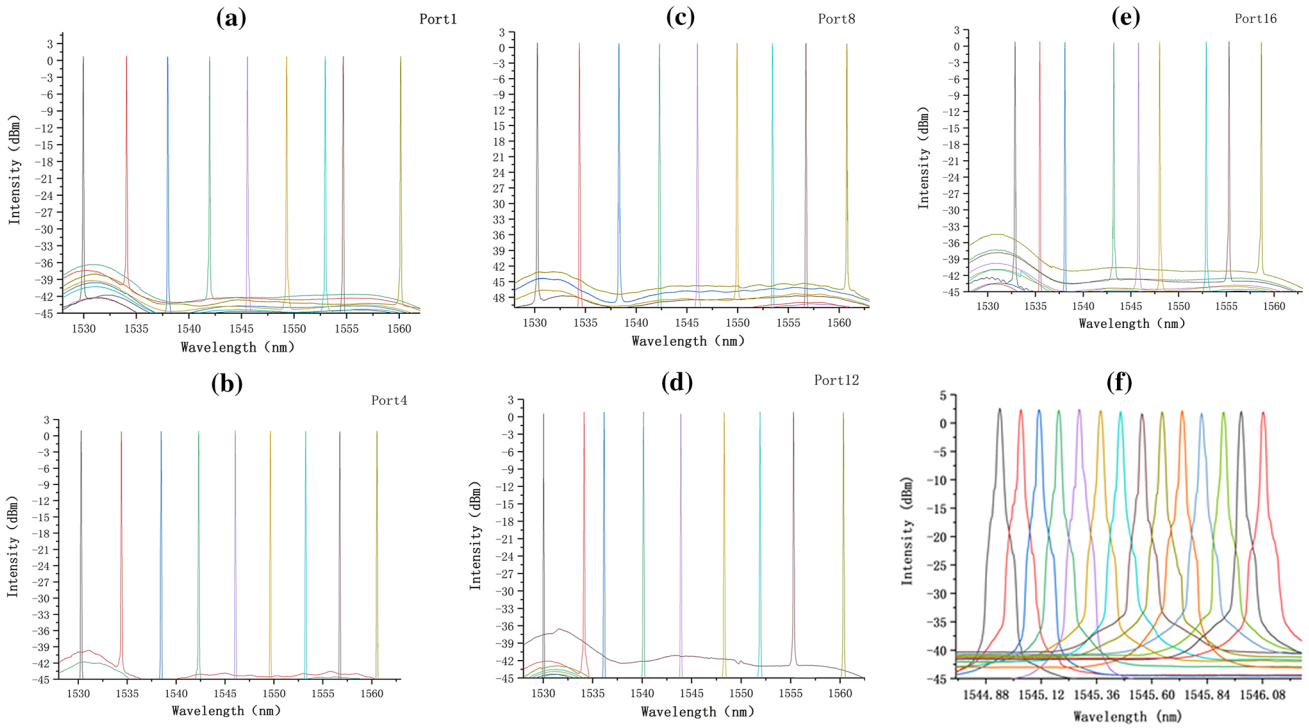

Fig. 7 **a**–**e** Coarse tuning characteristics in the C-band from tunable fiber lasers from ports 1, 4, 8, 12 and 16. **f** Fine wavelength tuning

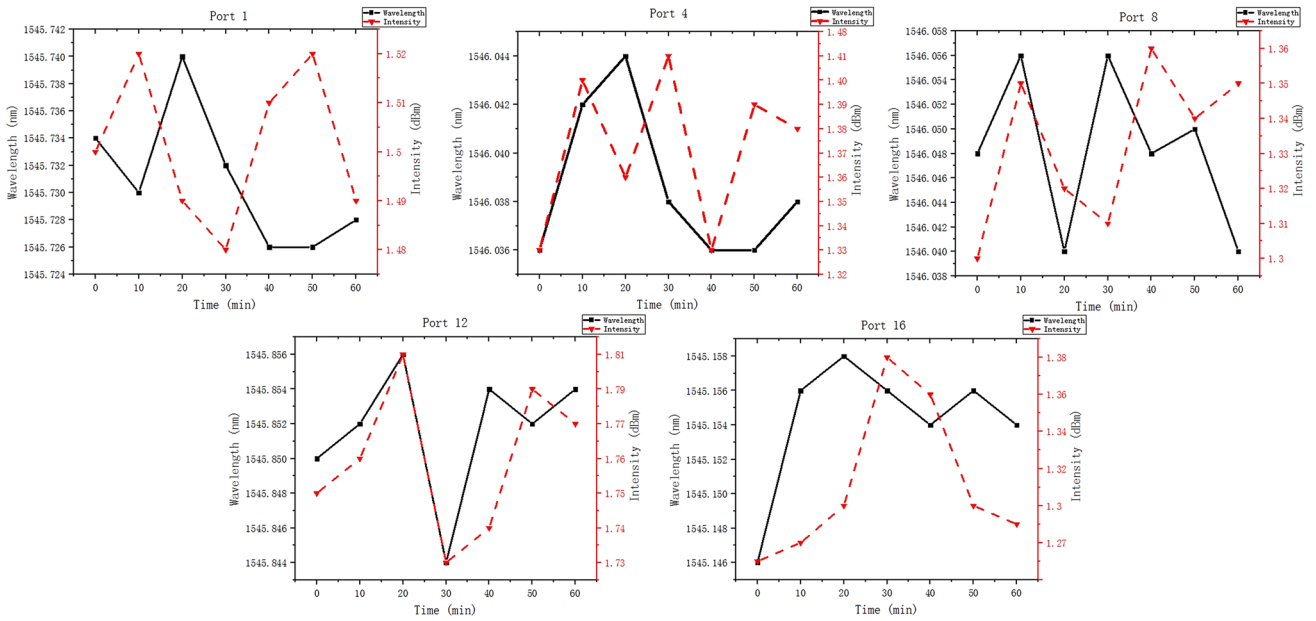

Fig. 8 Shift of center wavelength (solid line) and fluctuation of laser power (dotted line) from ports 1, 4, 8, 12 and 16 within 1 h, respectively

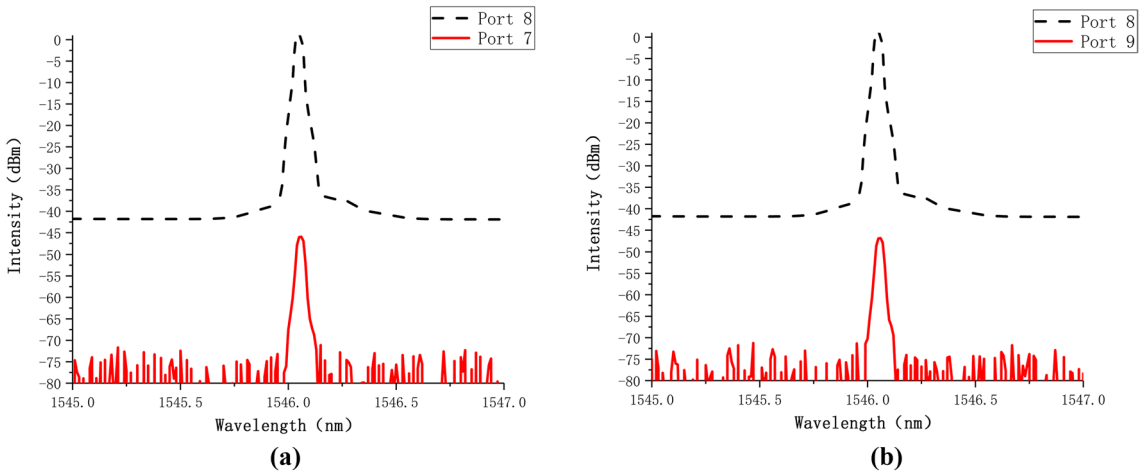

Fig. 9 Crosstalk measured at port 7 (**a**) and port 9 (**b**) when the laser output is from port 8

networks, which makes it very attractive for commercial use in the future.

Acknowledgements We acknowledge the financial support from the National Science Foundation of China (Grant no. 61675238), and National Key Scientific Instrument and Equipment Development Project (Grant no. 61627814).

References

1. J.Y. Wu, T. Pan, P. Cao, X.F. Hu, L.P. Jiang, X.H. Jiang, Y.K. Su, Compact wavelength blocker based on silicon microring resonator with nested pair of subrings. Opto-electronics and communication conference and Australian Conference on Optical Fibre Technology, Melbourne, VIC, pp. 563–565 (2014)
2. X.L. Fan, W. Zhou, S.M. Wang, X. Liu, Y. Wang, D.Y. Shen, Compact dual-wavelength thulium-doped fiber laser employing a double-ring filter. Appl. Opt. **55**, 3319–3322 (2016)
3. C.S. Kim, R.M. Sova, J.U. Kang, Tunable multiwavelength all-fiber Raman source using fiber Sagnac loop filter. Opt. Commun. **218**, 291–295 (2003)
4. C.C. Lee, S. Chi, Single-longitudinal-mode operation of a grating-based fiber-ring laser using self-injection feedback. Opt. Lett. **25**, 1774–1776 (2000)
5. Y. Zhao, J. Chang, Q.P. Wang, J.S. Ni, Z.Q. Song, H.F. Qi, C. Wang, P.P. Wang, L. Gao, Z.H. Sun, G.P. Lv, T.Y. Liu, G.D. Peng, Research on a novel composite structure Er^{3+}-doped DBR fiber laser with a π-phase shifted FBG. Opt. Exp. **21**, 22515–22522 (2013)

6. B. Zhou, H.H. Jiang, R.Z. Wang, C.T. Lu, Optical fiber Fabry–Perot filter with tunable cavity for high-precision resonance wavelength adjustment. J. Lightwave Technol. **33**, 2950–2954 (2015)
7. C.H. Yeh, F.Y. Shih, C.H. Wang, C.W. Chow, S. Chi, Cost-effective wavelength-tunable fiber laser using self-seeding Fabry–Perot laser diode. Opt. Exp. **16**, 435–439 (2008)
8. W. Yang, Y. Liu, L.F. Xiao, Z.X. Yang, Wavelength-tunable Erbium-doped fiber ring laser employing an acousto-optic filter. J. Lightwave Technol. **28**, 118–122 (2010)
9. S. Calvez, X. Rejeaunier, P. Mollier, J.-P. Goedgebuer, W.T. Rhodes, Erbium-doped fiber laser tuning using two cascaded unbalanced Mach–Zehnder Interferometers as intracavity filter: numerical analysis and experimental confirmation. J. Lightwave Technol. **19**, 893–898 (2001)
10. Y. Sakurai, M. Kawasugi, Y. Hotta, M.D. Saad Khan, H. Oguri, K. Takeuchi, S. Michihata, N. Uehara, LCOS-based wavelength blocker array with channel-by-channel variable center wavelength and bandwidth. IEEE Photon. Technol. Lett. **23**, 989–991 (2011)
11. D. Sinefeld, D.M. Marom, Tunable fiber ring laser with an intracavity high resolution filter employing two-dimensional dispersion and LCoS modulator. Opt. Lett. **37**, 1–3 (2012)
12. B. Robertson, H. Yang, M.M. Redmond, N. Collings, J.R. Moore, J. Liu, A.M. Jeziorska-Chapman, M. Pivnenko, S. Lee, A. Wonfor, I.H. White, W.A. Crossland, D.P. Chu, Demonstration of multi-casting in a 1×9 LCOS wavelength selective switch. J. Lightwave Technol. **32**, 402–410 (2014)
13. F. Xiao, K. Alameh, T. Lee, Opto-VLSI-based tunable single-mode fiber laser. Opt. Exp. **17**, 18676–18680 (2009)
14. Q. Ai, X. Chen, M. Tian, B.B. Yan, Y. Zhang, F.J. Song, G.X. Chen, X.Z. Sang, Y.Q. Wang, F. Xiao, K. Alameh, Demonstration of multi-wavelength tunable fiber lasers based on a digital micromirror device processor. Appl. Opt. **54**, 603–607 (2015)
15. D. Zhang, B.B. Yan, K.Z. Huang, Q. Yang, X. Chen, G.X. Chen, X.Z. Sang, Opto-DMD-based tunable triple-channel-wavelength fiber laser. *Optoelectronic Devices & Integration IV*. International Society for Optics and Photonics (2012)
16. X. Chen, B.B. Yan, F.J. Song, Y.Q. Wang, F. Xiao, K. Alameh, Diffraction of digital micromirror device gratings and its effect on properties of tunable fiber lasers. Appl. Opt. **51**, 7214–7220 (2012)
17. A. Billaud, P.C. Shardlow, W.A. Clarkson, Wavelength-flexible thulium-doped fiber laser employing a digital micro-mirror device tuning element. Conference on lasers and electro-optics (CLEO), San Jose, CA, pp. 1–2 (2016)
18. M.M. Tao, B. Tao, Z.Y. Hu, G.B. Feng, X.S. Ye, J. Zhao, Development of a 2 μm Tm-doped fiber laser for hyperspectral absorption spectroscopy applications. Opt. Exp. **25**, 32386–32394 (2017)